Pixel Dependent Automatic Parameter Selection for Image Denoising with Bilateral Filter

C. Shyam anand
Dept. of EEE, Indian Institute of Technology Guwahati, Guwahati, Assam, India

J. S. Sahambi
Dept. of EEE, Indian Institute of Technology Guwahati, Guwahati, Assam, India

ABSTRACT
Image denoising using bilateral filter is controlled by the width of its smoothing functions namely the domain and the range components. The choice of the width of range function is image dependent and requires several experiments. This paper presents an automatic method based on power-law scaling of the inverse of local statistics for pixel wise estimation of range parameter. This leads to an adaptive range function that is narrow along the edges and wide for smooth regions. The experimental results validate the performance of the proposed method of parameter selection in denoising images corrupted by additive white Gaussian noise.

General Terms
Image Denoising, Adaptive Bilateral Filter.

Keywords
Automatic parameter selection, bilateral filter, denoising, local statistics, pixel adaptive.

1. INTRODUCTION
The main objective of the advanced techniques in image denoising is to preserve the structural details while removing the noise. This is achieved by employing locally adaptive nonlinear filters that depend on the image characteristics. The adaptive filtering limits smoothing along the edges and thus reduces blurring. Therefore, these can also be referred as edge-preserving adaptive filters.

Methods like anisotropic diffusion, weighted least squares and robust statistics are among the iterative procedures for adaptive filtering of noise [1]. The bilateral filter originally developed by Tomasi et al [2] is a non-iterative method and it gives qualitatively better results than the iterative methods [3]. However, Elad [1] and Barash [4] have shown that bilateral filter and other adaptive filters are fundamentally related. Therefore, the simplicity and flexibility of bilateral filters extends its application in various contexts such as image denoising, contrast enhancement, super resolution, etc [3, 5, and 6].

The bilateral filter consists of two Gaussian weighting functions defined as the domain and the range component. The domain component characterizes the spatial distance and the range component signifies the intensity differences between the pixels defined within a neighbourhood. Basically, the performance of bilateral filter depends on the choice of the width of its smoothing kernels. In previous works [1–4, 7, 8], the widths of the smoothing kernels are chosen experimentally to suit the application. It is also shown that the range component is more decisive than the domain component and its width should be adapted to the noise level for better denoising [7–10].

Liu et al [7] adapted the width of the range kernel to local noise variance estimates for improving the denoising efficiency of bilateral filter and is chosen as 1.95 times of the local noise level. Zhang [8] studied the optimal choice of kernel widths as a function of noise variance. It is verified that the optimal width of range kernel is linearly related to the noise level and is chosen as 1.7 times of the global noise variance. Wong [9] proposed a method to adaptively vary the parameters of bilateral filter based on the local phase characteristics of the image to be denoised. As a result, smoothing in the high contrast regions is limited relative to the smooth regions. However, it requires the range of the filter parameters to be determined experimentally similar to the standard bilateral filter. Rose et al [11] proposed a method to vary the range parameter of the bilateral filter based on the standard deviation of noise.

In this paper, we address the issues in choosing the width of the range kernel and show that it can be determined automatically from the local statistics of the image. The proposed method results in pixel wise adaptation of the filter width. The experimental results show that the proposed method for automatic and pixel wise estimation of the range filter width gives qualitatively similar and possibly improved results for higher noise levels. The experiments were performed on gray scale and colour images.

The rest of the paper is organized as follows: Section 2 discusses about the bilateral filter parameters and presents the proposed method for automatic and pixel wise parameter selection. In Section 3, the experimental results comparing the performance of the proposed method for denoising various images under various noise levels are discussed in detail. Section 4 concludes the paper stating the advantages and the limitations of the proposed method.

2. BILATERAL FILTER WITH AUTOMATIC PARAMETER SELECTION
Define a 2D discrete image f_{xy} of size $N \times N$, such that $\{x, y\} \in \{0,...N-1\} \times \{0,...N-1\}$. Assume that f_{xy} is corrupted by additive white Gaussian noise of variance σ_n^2. The denoised image $\hat{f}_{xy}$ obtained using the bilateral filter is defined as

$$\hat{f}_{xy} = \frac{1}{C}\sum_{i=x-d}^{x+d}\sum_{j=y-d}^{y+d} W_s(i;x,j;y)W_r(f_{ij};f_{xy})f_{ij} \quad (1)$$

Where, d is a non-negative integer such that $(2d+1)\times(2d+1)$ denotes the neighborhood window size. W_s and W_r are the domain and range components respectively and are defined as

$$W_s(i;x,j;y) = \exp\left(-\frac{\left|(i-x)^2+(j-y)^2\right|}{2\sigma_s^2}\right) \quad (2)$$

and

$$W_r(f_{ij};f_{xy}) = \exp\left(-\frac{\left|f_{ij}-f_{xy}\right|^2}{2\sigma_r^2}\right). \quad (3)$$

The normalization constant C is given as

$$C = \frac{1}{\sum_{i=x-d}^{x+d}\sum_{j=y-d}^{y+d} W_s(i;x,j;y)W_r(f_{ij};f_{xy})}. \quad (4)$$

The parameters σ_s^2 and σ_r^2 are the variances that specify the width of the domain and range kernels respectively.

The optimal performance of the bilateral filter depends on the choice of σ_s and σ_r [8]. Hence, they are considered as the controlling parameters. From the definition in (2) it can be inferred that the domain component is independent of the image content. Its influence depends only on the spatial distance between the pixels and not on their intensity values. Conversely, the range component defined in (3) depends on the intensity values and hence, it decreases the influence of pixels at (i,j) when their intensity values differ from f_{xy}. This implies that the range component adapts to the structural content of the image and therefore, the extent of filtering is more influenced by the choice of σ_r [10]. It can be understood that large noise levels require higher values of σ_r and vice-versa. This dependency leads to the proportionality,

$$\sigma_r = \lambda\sigma_n. \quad (5)$$

λ is the constraint parameter that determines the value of σ_r. Large value of λ will over smooth the image and small values will not suppress noise properly. Generally, the optimal value of λ is chosen experimentally such that there remains a trade-off between image smoothing and its sharpness. However, this approach has the following setbacks.

(1) It demands several experiments to obtain an optimal λ for image denoising. Since its choice is independent of image characteristics it may not be optimal for all the images corrupted by various noise levels.

(2) λ is a scalar resulting in a single choice of σ_r. It means that the level of smoothing is uniform over the entire image. Thus it assumes that the influence of noise is independent of the image content. But real images almost always violate this assumption.

The noise in smooth regions is perceptually more dominant than in the edges and coarse texture regions. This requires comparatively less smoothing along the edges and the coarse details [12]. This problem can be handled by varying the control parameter σ_r (and so λ) from pixel to pixel. This is done using the local statistics of the image to be denoised.

The local mean (variance) of a pixel f_{xy} is computed locally over its neighbourhood of size $(2d+1)\times(2d+1)$. The mean of a pixel m_{xy} is defined as [13]

$$m_{xy} = \frac{1}{(2d+1)^2}\sum_{i=x-d}^{x+d}\sum_{j=y-d}^{y+d} f_{ij}. \quad (6)$$

Similarly the variance of a pixel σ_{xy}^2 is obtained from

$$\sigma_{xy}^2 = \frac{1}{(2d+1)^2}\sum_{i=x-d}^{x+d}\sum_{j=y-d}^{y+d}\left(f_{ij}-m_{xy}\right)^2 \quad (7)$$

In the case of colour images the variance of a pixel is considered as the average of the variances computed from the RGB components.

The pixels belonging to the high contrast regions such as edges and coarse texture regions have high variance and those belonging to smooth regions have low variance values [12]. Since the objective is to restrict λ along the high contrast regions it is assumed that

$$\lambda_{xy} = \frac{max(\sigma_{xy})}{\sigma_{xy}} \quad (8)$$

The locally computed variance varies directly as its mean and so there exists large variations in the value of λ corresponding to pixels in the low and high contrast regions. Hence, power-law transformation is performed to stabilize the dynamic range and scale the values of λ [14]. Therefore, the value of σ_r for each pixel at (x,y) is obtained as

$$(\sigma_r)_{xy} = (\lambda_{xy})^{\gamma}\sigma_n. \quad (9)$$

The value of parameter γ controls the degree of smoothing. The resultant σ_r is a matrix of control values that varies according to the pixel characteristics and is also properly balanced among the pixels belonging to smooth regions, edges and coarse texture regions. The range component in (3) can therefore be redefined as,

$$W_r(f_{ij};f_{xy}) = \exp\left(-\frac{\left|f_{ij}-f_{xy}\right|^2}{2(\sigma_r^2)_{xy}}\right). \quad (10)$$

3. RESULTS AND DISCUSSION

The performance of the proposed method is verified by conducting experiments on the standard test images. The images included in the experiment are mentioned in Table 1. The evaluations are also performed on magnetic resonance (MR) images in order to validate the application of the proposed method in medical image denoising.

The noisy image $\hat{f}$ is generated by adding white Gaussian noise of variance σ_n^2 to the original image f and is simulated using MATLAB as follows [15]:

$$\bar{f} = f + [\sigma_n \times randn(size(f))] \quad (11)$$

The value of σ_n is assumed to lie within the range [0.01− 0.1]. The optimal neighbourhood size for computing the local variance and the response of the filter is experimentally determined as 11×11. The optimal value of domain parameter σ_s is evaluated as 3. The empirical value of power variable γ in (9) is estimated as $9\sigma_n$ for gray scale images and $4\sigma_n$ for color images.

The values of the range parameter σ_r computed for each pixel of the noisy Barbara image is shown in Figure 1(a). It can be verified that the σ_r values corresponding to the edge pixels are less than the pixels in flat regions and also the range parameter value for each edge pixel depends on its strength. This is because the strong edges are less influenced by noise than the weak edges. As a result the variance of the strong edge pixels is high and weak edges are characterized by comparatively low variance values. Thus the degree of smoothing along the strong edges is relatively less than the weak edges.

From the experiments it is observed that as the noise level increases the local variance in the flat regions increases substantially than in the edges. This can also be verified from the plot in Figure 1(b). For this reason the slope of the power-law transformation should decrease for high values of σ_n. As a result the range of $(\sigma_r)_{xy}$ values corresponding to the pixels $f(x, y)$ in the flat regions will be expanded to ensure sufficient smoothing. Figure 1(c) gives the plot of control values $(\sigma_r)_{xy}$ obtained for the local variances shown in Figure 1(b). From these plots it is obvious that for high noise levels the increase in range values $(\sigma_r)_{xy}$ for the edges and coarse texture regions are well regulated. Similarly, the range values for the smooth regions are sufficiently boosted to ensure proper smoothing.

The effectiveness of the proposed technique for improving the bilateral filter is validated using the root mean square error (RMSE) and the structural similarity (SSIM) index [16]. The value of SSIM index lies between [-1, 1]. Minimum values of RMSE and large values of SSIM index mean high similarity between the compared images.

The results of parameter selection obtained for the experiments performed on the test images for various noise levels are given in Table 1. From this it can be understood that the values of σ_r (both in fixed and adaptive) increases with the noise level to ensure sufficient smoothing. In the case of fixed σ_r as employed in standard bilateral filter [2]; the increase had to be limited to retain the image sharpness. As a result smoothing in flat region will be compensated. Conversely, the adaptive choice allocates higher σ_r in the flat regions in spite of limited σ_r in the edges. Thus it achieves good smoothing and retains image sharpness. Also, for low noise levels the range between σ_r for edges and flat regions is well controlled, such that there is no excess smoothing.

This improvement is confirmed by comparing the values of quality metrics RMSE and the SSIM index given in Table 2. It can be verified that the proposed adaptive parameter estimation strategy yields better results for most of the test images and is particularly higher for increasing noise levels. In the case of Mandrill image the improvement is not as expected. This is because most of the regions in this image are coarse texture regions. Due to the dependence of the proposed method on local variance values, the estimated σ_r for the pixels in these regions were slightly higher. However, the minimal difference in the values of SSIM indicates that the variations will not be perceptually significant. The image denoising results obtained for some of the test images are shown in Figure 2 for visual inspection.

4. CONCLUSSION

This paper presents a simple and intuitive approach for pixel wise adaptation of the smoothing values based on the local variance and thus directs towards automatically tuning the control parameter σ_r of the bilateral filter. The experimental results prove that the proposed approach also improves the denoising efficiency of the bilateral filter. This method can be further improved by using adaptive neighborhoods of variable size and shape in order to estimate the local variances and the filter response.

The results are presented for noise levels $\sigma_n \leq 0.1$. However, in the case of $\sigma_n > 0.1$ the value of γ becomes ≥ 1 for which the power-law transformation further reduces the value of λ_{xy} corresponding to the edge regions. Hence, the level of smoothing along the edges is decreased preserving few noise pixels. This problem limits the advancement of the proposed approach for very low signal to noise ratio images with $\sigma_n > 0.1$. One possible solution for this problem would be to apply the transformation independently for the edges and the smooth regions specifying different value of γ respectively.

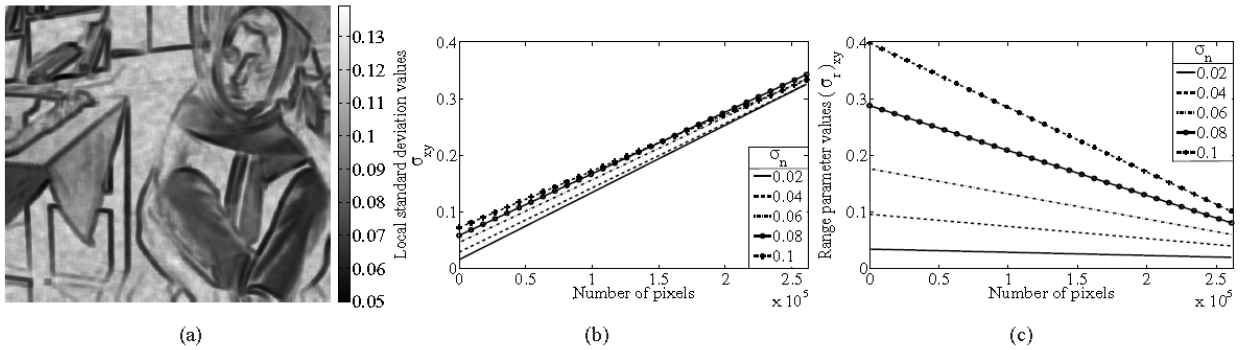

(a) (b) (c)

Figure 1: Results for Barbara image: (a) Illustration of pixel wise allocation of σ_r values for $\sigma_n = 0.05$ (b) Plot of local standard deviation σ_{xy} estimated for different noise levels. (c) Plot of range parameter values σ_r estimated corresponding to the σ_{xy} values in (b).

Table 1: Fixed and adaptive range parameter σ_r estimated for different test images. [a,b] denote the interval of adaptive σ_r

Range parameter values for gray scale images								
	Barbara		Cameraman		Pattern		MR image	
σ_n	Fixed σ_r	Adaptive σ_r	Fixed σ_r	Adaptive σ_r	Fixed σ_r	Adaptive σ_r	Fixed σ_r	Adaptive σ_r
0.01	0.015	[0.01, 0.0137]	0.0075	[0.01, 0.0141]	0.0150	[0.01, 0.0156]	0.015	[0.01, 0.0178]
0.03	0.0525	[0.03, 0.0609]	0.045	[0.03, 0.0652]	0.0525	[0.03, 0.0857]	0.0675	[0.03, 0.0741]
0.05	0.0975	[0.05, 0.1393]	0.0975	0.05, 0.1506]	0.1375	[0.05, 0.2194]	0.125	[0.05, 0.1827]
0.07	0.1505	[0.07, 0.2226]	0.175	[0.07, 0.2827]	0.2100	[0.07, 0.4562]	0.175	[0.07, 0.3215]
0.10	0.25	[0.10, 0.4260]	0.275	[0.10, 0.5755]	0.35	[0.10, 1.0050]	0.275	[0.10, 0.7307]
Range parameter values for color images								
	Mandrill		Lena		Peppers		House	
σ_n	Fixed σ_r	Adaptive σ_r	Fixed σ_r	Adaptive σ_r	Fixed σ_r	Adaptive σ_r	Fixed σ_r	Adaptive σ_r
0.01	0.01	[0.01, 0.0112]	0.01	[0.01, 0.0114]	0.01	[0.01, 0.0118]	0.0125	[0.01, 0.0119]
0.03	0.03	[0.03, 0.0406]	0.0375	[0.03, 0.0402]	0.0375	[0.03, 0.0449]	0.045	[0.03, 0.0408]
0.05	0.05	[0.05, 0.0770]	0.075	[0.05, 0.0745]	0.075	[0.05, 0.0805]	0.075	[0.05, 0.0754]
0.07	0.07	[0.07, 0.1177]	0.1225	[0.07, 0.1305]	0.1225	[0.07, 0.1242]	0.1225	[0.07, 0.1147]
0.1	0.1	[0.10, 0.1930]	0.2	[0.10, 0.2024]	0.2	[0.10, 0.2022]	0.2	[0.10, 0.1767]

Table 2: Comparison of RMSE and SSIM values obtained for denoising test images using fixed and adaptive choice of σ_r

Results for gray scale images																
	Barbara				Cameraman				Pattern				MR image			
σ_n	Fixed σ_r		Adaptive σ_r		Fixed σ_r		Adaptive σ_r		Fixed σ_r		Adaptive σ_r		Fixed σ_r		Adaptive σ_r	
	RMSE	SSIM	RMSE	SSIM	RMSE	SSIM	RMSE	SSIM	RMSE	SSIM	RMSE	SSIM	RMSE	SSIM	RMSE	SSIM
0.01	0.0098	0.9867	0.0094	0.9863	0.0090	0.9883	0.0084	0.9879	0.0046	0.9968	0.0049	0.9960	0.0076	0.9914	0.0071	0.9909
0.03	0.0268	0.9426	0.0235	0.9422	0.0228	0.9526	0.0194	0.9553	0.0098	0.9860	0.0098	0.9887	0.0201	0.9543	0.0182	0.9550
0.05	0.0408	0.8949	0.0346	0.8995	0.0348	0.9144	0.0287	0.9199	0.0158	0.9697	0.0152	0.9774	0.0296	0.8974	0.0275	0.9005
0.07	0.0555	0.8477	0.0468	0.8579	0.0520	0.8788	0.0385	0.8834	0.0242	0.9544	0.0205	0.9576	0.0385	0.8279	0.0384	0.8280
0.1	0.0678	0.7891	0.0605	0.8084	0.0710	0.8234	0.0549	0.8297	0.0410	0.9209	0.0300	0.9359	0.0594	0.7656	0.0536	0.7776
Results for color images																
	Mandrill				Lena				Peppers				House			
σ_n	Fixed σ_r		Adaptive σ_r		Fixed σ_r		Adaptive σ_r		Fixed σ_r		Adaptive σ_r		Fixed σ_r		Adaptive σ_r	
	RMSE	SSIM	RMSE	SSIM	RMSE	SSIM	RMSE	SSIM	RMSE	SSIM	RMSE	SSIM	RMSE	SSIM	RMSE	SSIM
0.01	0.0098	0.9950	0.0099	0.9949	0.0081	0.9905	0.0081	0.9904	0.0096	0.9900	0.0099	0.9896	0.0093	0.9909	0.0090	0.9914
0.03	0.0248	0.9659	0.0252	0.9643	0.0159	0.9600	0.0158	0.9603	0.0208	0.9541	0.0205	0.9542	0.0188	0.9537	0.0175	0.9601
0.05	0.0351	0.9264	0.0358	0.9216	0.0214	0.9350	0.0211	0.9352	0.0266	0.9285	0.0260	0.9287	0.0231	0.9360	0.0226	0.9367
0.07	0.0433	0.8833	0.0442	0.8752	0.0260	0.9144	0.0253	0.9160	0.0308	0.9099	0.0299	0.9093	0.0281	0.9171	0.0268	0.9174
0.1	0.0543	0.8152	0.0552	0.8064	0.0322	0.8880	0.0308	0.8909	0.0359	0.8860	0.0345	0.8866	0.0355	0.8881	0.0333	0.8885

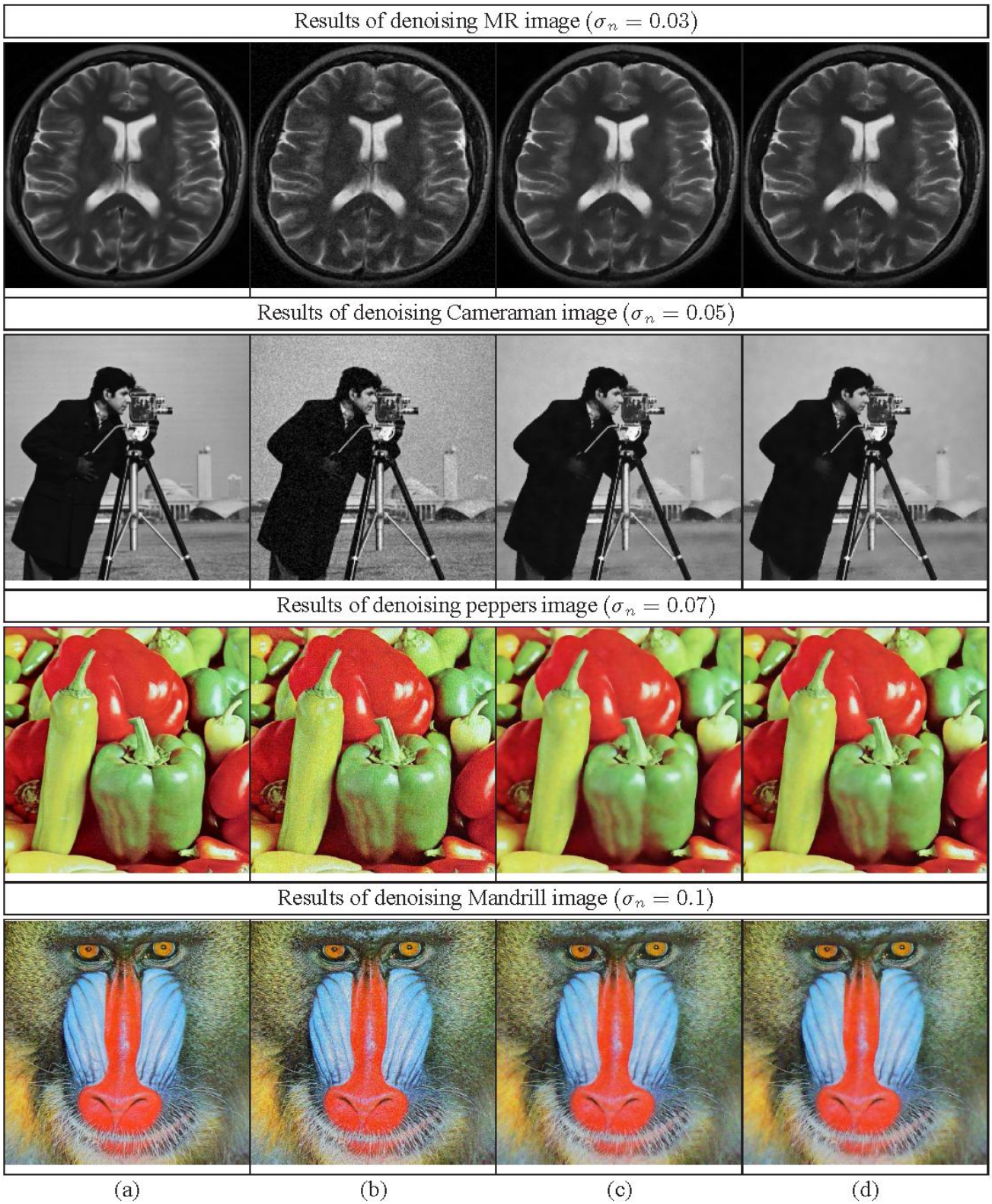

Figure 2: Illustration of image denoising results. In column: (a) Original images (b) Noisy images (c) Denoising results using bilateral filter with fixed σ_r (d) Denoising results using bilateral filter with automatically estimated pixel wise σ_r values.

5. REFERENCES

[1] M. Elad, "On the Origin of the Bilateral Filter and Ways to Improve it," *IEEE Transaction on Image Processing*, vol. 11, no. 10, pp. 1141–1151, October 2002.

[2] C. Tomasi and R. Manduchi, "Bilateral Filtering for Gray and Color Images," in *Proc. 6th Int. Conf. Computer Vision*, 1998, pp. 839–846.

[3] S. Paris, P. Kornprobst, J. Tumblin, and F. Durand, *Bilateral Filtering: Theory and Applications*, *Foundations and Trends in Computer Graphics and Vision*. Now publishers Inc., 2008, vol. 4, no. 1.

[4] D. Barash, "A Fundamental Relationship between Bilateral Filtering, Adaptive Smoothing, and the Nonlinear Diffusion Equation," *IEEE Transaction on Pattern Analysis and Machine Intelligence*, vol. 24, no. 6, pp. 844–847, June 2002.

[5] J.-W. Han, J.-H. Kim, S.-H. Cheon, and J.-O. Kim, "A Novel Image Interpolation Method Using the Bilateral Filter," *IEEE Transactions on Consumer Electronics*, vol. 56, no. 1, pp. 175–181, Feb. 2010.

[6] L. Qiegen, L. Jianhua, and Z. Yuemin, "Adaptive Image Decomposition by Improved Bilateral Filter," *International Journal of Computer Applications*, vol. 23, pp. 16–22, 2011.

[7] C. Liu, W. T. Freeman, R. Szeliski, and S. B. Kang, "Noise Estimation from a Single Image," *IEEE Computer Society Conference on Computer Vision and Pattern Recognition*, vol. 1, pp. 901–908, 2006.

[8] M. Zhang and B. K. Gunturk, "Multiresolution Bilateral Filtering for Image Denoising," *IEEE Transactions on Image Processing*, vol. 17, no. 12, pp. 2324–2333, Dec. 2008.

[9] A. Wong, "Adaptive bilateral filtering of image signals using local phase characteristics," *Signal Processing*, vol. 88, no. 6, pp. 1615–1619, June 2008.

[10] B. Zhang and J. P. Allebach, "Adaptive Bilateral Filter for Sharpness Enhancement and Noise Removal," *IEEE Transactions on Image Processing*, vol. 17, no. 5, pp. 664–678, May 2008.

[11] A. Gabiger-Rose, M. Kube, P. Schmitt, R. Weigel, and R. Rose, "Image denoising using bilateral filter with noise-adaptive parameter tuning," in *IECON 2011*. IEEE Industrial Electronics Society, Nov. 2011, pp. 4515–4520.

[12] J. Lee, "Refined Filtering of Image Noise using Local Statistics," *Computer Graphics and Image Processing*, vol. 15, pp. 380–389, 1981.

[13] J.-S. Lee, "Digital Image Enhancement and Noise Filtering by use of Local Statistics," *IEEE Transactions on Pattern Analysis and Machine Intelligence.*, vol. 2, no. 2, pp. 165–168, March 1980.

[14] R. C. Gonzalez, *Digital Image Processing*, 2nd ed. Pearson Education, 2004.

[15] P. C. Hansen, J. G. Nagy, and D. P. O'Leary, *Deblurring Images: Matrices, Spectra, and Filtering (Fundamentals of Algorithms 3)*. SIAM, 2006.

[16] Z. Wang, A. C. Bovik, H. R. Sheikh, and E. P. Simoncelli, "Image quality assessment: From error visibility to structural similarity," *IEEE Transactions on Image Processing*, vol. 13, no. 4, pp. 600–612, April 2004